complexes may be attributed to the more rigid $(pd)_2V$ geometry, decreased V–CO π-back-bonding, or reduced spin delocalization, all of which make the metal center less susceptible to nucleophilic attack.

Acknowledgment. We thank the National Science Foundation for support of this research. We also thank Nong Liang (Northwestern University) for assistance with flash photolysis experiments.

The Oscillatory Landolt Reaction. Empirical Rate Law Model and Detailed Mechanism

Vilmos Gáspár[1] and Kenneth Showalter*

Contribution from the Department of Chemistry, West Virginia University, Morgantown, West Virginia 26506-6045. *Received October 30, 1986*

Abstract: The iodate oxidation of sulfite and ferrocyanide when carried out in a continuous flow stirred tank reactor exhibits large-amplitude oscillations in pH accompanied by an almost constant concentration of iodide. A description of the reaction in terms of component processes and associated empirical rate laws is used to model the dynamical behavior. Limitations and potential refinements of the empirical rate law model are discussed. A detailed mechanism consistent with the component process description is presented.

Just over one hundred years ago, Landolt reported on his studies of the iodate oxidation of sulfite.[2] His careful investigation yielded an empirical expression for the time of appearance of molecular iodine upon complete consumption of sulfite as a function of reactant concentrations and temperature, which is still used for the "Landolt clock reaction" classroom demonstration.[3] A detailed study published in 1921 by Eggert and Scharnow[4] extended Landolt's investigation of the oxidation of sulfite and also reported on the oxidations of ferrocyanide and arsenous acid. Their study was the first to recognize the autocatalytic nature of these reactions. More recently, the reaction with arsenite has served as a model system for the study of bistability[5-10] and propagating reaction–diffusion fronts.[11-14]

In a recent dramatic discovery, Edblom, Orbán, and Epstein[15] (EOE) found oscillatory behavior in the iodate oxidation of sulfite in a stirred flow reactor (CSTR) when ferrocyanide was also included as a reactant. Large-amplitude oscillations in pH and potential of a Pt electrode were measured. The highly temperature sensitive behavior is characterized by a cross-shaped phase diagram[16,17] showing the reactor residence times and feed concentrations of $Fe(CN)_6^{4-}$ where monostability, bistability, and oscillations are exhibited.

Table I. Reactant Stream Composition

$[KIO_3]_0$[a] = 7.5×10^{-2} M	$[Na_2SO_3]_0 = 8.93 \times 10^{-2}$ M
$[K_4Fe(CN)_6]_0 = 2.5 \times 10^{-2}$ M	$[H_2SO_4]_0 = 3.5 \times 10^{-3}$ M

[a] $[I^-]_0 = 7.5 \times 10^{-7}$ M, based on analysis of iodate reagent.

Oligo-oscillatory behavior in the batch reaction of iodate with sulfite and malonic acid has been reported by Beck et al.[18,19] Three damped extrema in the concentration of iodide are exhibited before the final approach to the equilibrium composition. The discovery by EOE[15] represents the first example of sustained oscillations in a Landolt type system. While bistability is exhibited in the related iodate oxidation of arsenous acid, no evidence of oscillatory behavior has been found in this system with buffered[15,20] or unbuffered solutions.[21] That oscillations are exhibited in the iodate oxidation of a mixture of sulfite and ferrocyanide points to subtle but important differences in the reaction of iodate with various reducing agents.

In this paper we report on additional experimental characterization and mechanism analysis of the oscillatory iodate oxidation of sulfite and ferrocyanide. Our analysis relies on reactions proposed by Landolt,[2] Eggert and Scharnow,[4] and EOE,[15] together with empirical rate laws and associated rate constants for the component processes. From these sources we develop a simple empirical rate law (ERL) model that reproduces the qualitative and in some cases nearly quantitative dynamical behavior of the system. The ERL model is tested by comparing experimental and

(1) Permanent address: Department of Physical Chemistry, Kossuth Lajos University, H-4010 Debrecen, Hungary.
(2) Landolt, H. *Ber. Dtsch. Chem. Ges.* **1886**, *19*, 1317.
(3) Schroeter, L. C. *Sulfur Dioxide*; Pergamon Press: New York, 1966; pp 80–81.
(4) Eggert, J.; Scharnow, B. *Z. Elektrochem.* **1921**, *27*, 455.
(5) De Kepper, P.; Epstein, I. R.; Kustin, K. *J. Am. Chem. Soc.* **1981**, *103*, 6121.
(6) Papsin, G. A.; Hanna, A.; Showalter, K. *J. Phys. Chem.* **1981**, *85*, 2575.
(7) Ganapathisubramanian, N.; Showalter, K. *J. Phys. Chem.* **1983**, *87*, 1098, 4014.
(8) Ganapathisubramanian, N.; Showalter, K. *J. Chem. Phys.* **1984**, *80*, 4177.
(9) Pifer, T.; Ganapathisubramanian, N.; Showalter, K. *J. Chem. Phys.* **1985**, *83*, 1101.
(10) Ganapathisubramanian, N.; Showalter, K. *J. Chem. Phys.* **1986**, *84*, 5427.
(11) Gribschaw, T. A.; Showalter, K.; Banville, D. L.; Epstein, I. R. *J. Phys. Chem.* **1981**, *85*, 2152.
(12) Hanna, A.; Saul, A.; Showalter, K. *J. Am. Chem. Soc.* **1982**, *104*, 3838.
(13) Saul, A.; Showalter, K. In *Oscillations and Traveling Waves in Chemical Systems*; Field, R. J., Burger, M., Eds.; Wiley: New York, 1985; pp 419–439.
(14) Harrison, J.; Showalter, K. *J. Phys. Chem.* **1986**, *90*, 225.
(15) Edblom, E. C.; Orbán, M.; Epstein, I. R. *J. Am. Chem. Soc.* **1986**, *108*, 2826.
(16) Boissonade, J.; De Kepper, P. *J. Phys. Chem.* **1980**, *84*, 501.
(17) Epstein, I. R. *J. Phys. Chem.* **1984**, *88*, 187.
(18) Rábai, Gy.; Bazsa, Gy.; Beck, M. T. *J. Am. Chem. Soc.* **1979**, *101*, 6746.
(19) Beck, M. T.; Rábai, Gy. *J. Phys. Chem.* **1985**, *89*, 3907.
(20) Ganapathisubramanian, N.; Showalter, K. *J. Phys. Chem.* **1985**, *89*, 2118.
(21) Gáspár, V.; Showalter, K., unpublished results.

0002-7863/87/1509-4869$01.50/0

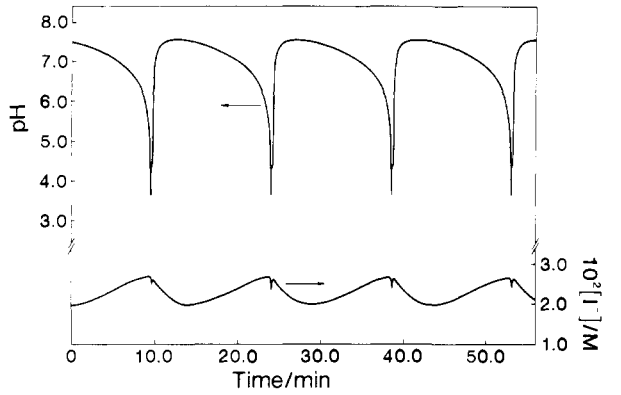

Figure 1. Iodide concentration (below) and pH (above) as a function of time. Reactant stream concentrations in Table I and $k_0 = 2.5 \times 10^{-3}$ s^{-1}. Temperature: 40.0 °C.

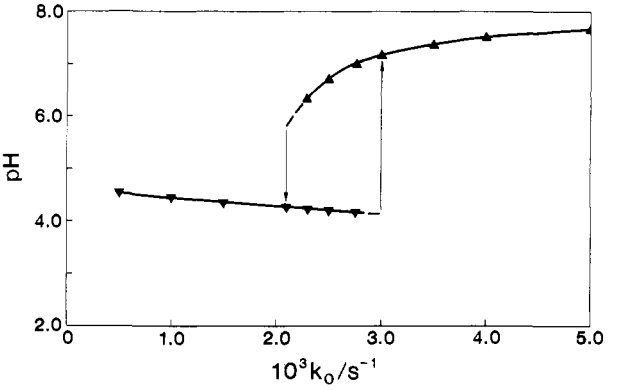

Figure 2. Steady state pH as a function of k_0; thermo branch (▼) and flow branch (▲). Reactant stream concentrations in Table I. Temperature: 30.0 °C.

calculated oscillation waveforms, constraint phase diagrams, and dependence of period and amplitude on feed steam acidity. In addition, we present a detailed mechanism of the reaction in terms of elementary steps, consistent with the ERL model. We refer to the CSTR iodate oxidation of sulfite and ferrocyanide as the *oscillatory Landolt reaction.*[22]

Edblom et al.[23] report on an independent study of the oscillatory Landolt reaction in the following paper. Their mechanism analysis, in terms of elementary steps, yields a characterization of the reaction that resembles the description presented here in all major aspects.

Experimental Section

Materials and Equipment. Stock solutions of KIO_3, Na_2SO_3, $K_4Fe(CN)_6$, and H_2SO_4 were prepared with doubly distilled water and reagent grade chemicals. The concentration of the H_2SO_4 solution was determined by titration against standard base. The concentration of the Na_2SO_3 solution was determined by reaction with I_2 generated from KIO_3 and excess KI in acidic solution and titration with standard $Na_2S_2O_3$ solution.[24] Reagent grade KIO_3 and $K_4Fe(CN)_6$ were considered primary standards,[24] and the concentrations of the corresponding stock solutions were determined by weight of dissolved chemical.

A machined Plexiglas CSTR, previously described,[6] was used with two Gilson Minipuls peristaltic pumps. Use of two pumps allowed independent calibration and adjustment of the input channels. Iodide concentration and pH were monitored with iodide-selective and pH electrodes and associated instrumentation (Orion and Fisher). Solutions were maintained homogeneous with a glass impeller turning at 900 rpm (Fisher Stedi-Speed) and temperature was monitored with use of a type K thermocouple (Omega).

Procedure. Reagent solutions, one containing KIO_3 and the other containing Na_2SO_3, $K_4Fe(CN)_6$, and H_2SO_4, were prepared volumetrically from the stock solutions. Reagent solutions were stored under argon gas throughout each experiment. Each channel was calibrated before each experiment with a volume-measurement flow meter (Phase Separation, Ltd.). The flow rate at a particular pump setting typically varied by less than 2% over the course of a day and the variation during any single experiment was negligible. The volume of the CSTR (35.7 mL) was determined kinetically by measuring iodide concentration as distilled water was pumped at a known rate into the tank initially filled with iodide solution. The apparent first-order rate constant (k_0 = flow rate/tank volume) for the decrease in iodide concentration allows calculation of the tank volume.

Experimental Behavior

Shown in Figure 1 are simultaneous measurements of pH and iodide concentration as a function of time over the course of several oscillations. These measurements were made at 40.0 °C with input concentrations listed in Table I. Hydrogen ion concentration changes by almost four orders of magnitude within a period, yet iodide concentration changes by less than 15% about its average.

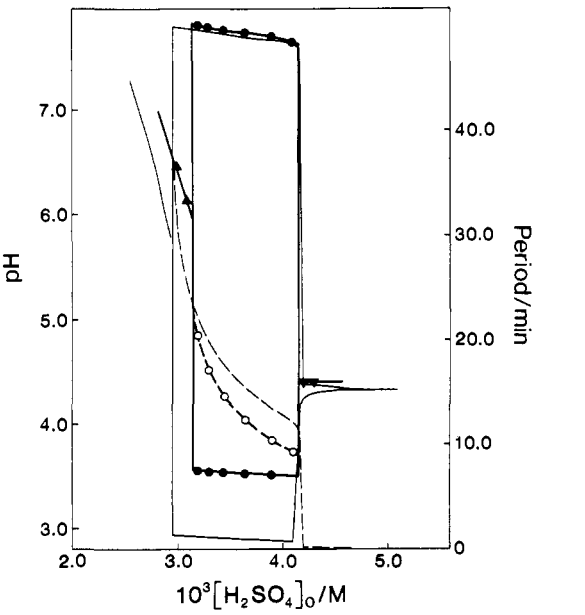

Figure 3. Measured amplitude (●) and period (○) of pH oscillations as a function of $[H_2SO_4]_0$ at 40.0 °C with $k_0 = 2.5 \times 10^{-3}$ s^{-1}. Reactant concentrations in Table I. Flow branch (▲) and thermo branch (▼) steady state pH shown bracketing oscillatory region. Amplitude (—) and period (- -) of pH oscillations calculated from model N. Reactant concentrations in Table I, rate constants in Table II, and $k_0 = 2.5 \times 10^{-3}$ s^{-1}. Calculated steady state pH (—) shown bracketing oscillatory region.

Large changes in pH and almost constant iodide concentrations were found in all measurements of the oscillatory behavior.

Also shown in Figure 1 are phase relations between pH and iodide concentration. The minimum in I^- concentration follows shortly after the minimum in H^+ concentration (pH maximum). As iodide concentration gradually increases from its minimum value, pH falls at an increasing rate to a sharp minimum. The minimum in pH nearly coincides with the first maximum in iodide concentration. A small negative spike in iodide concentration is then exhibited as pH sharply increases from its minimum value to a short plateau. The pH again rapidly increases from the plateau to the next maximum while iodide concentration falls from its second maximum to the next minimum.

Shown in Figure 2 are measurements of steady state pH as a function of k_0 with the same reactant concentrations as in Figure 1 but with the temperature at 30.0 °C. We now see bistability rather than oscillations. The thermodynamic (thermo) branch of steady states extends to the point of thermodynamic equilibrium at $k_0 = 0$; the flow branch extends to high values of k_0 where the reaction mixture composition approaches that of the combined reactant streams. The system may exist in either of the two possible steady states at any particular value of k_0 where the branches overlap; in which state the system resides depends on

(22) An alternative name for this system might be "the oscillatory Edblom, Orbán, Epstein (EOE) reaction" after its discoverers.
(23) Edblom, E. C.; Györgyi, L.; Orbán, M.; Epstein, I. R. *J. Am. Chem. Soc.* following paper in this issue.
(24) Kolthoff, I. M.; Belcher, R. *Volumetric Analysis*; Interscience: New York, 1957; Vol. 3, pp 292–294.

the pathway in reaching that state.

Shown in Figure 3 are the period and amplitude of the pH oscillations as a function of the reactant stream concentration of sulfuric acid, $[H_2SO_4]_0$. The amplitude remains almost constant throughout the oscillatory region; however, the period almost doubles between the bifurcation points at the extremes of the region. Also shown are steady states of the thermo branch at high $[H_2SO_4]_0$ and of the flow branch at low $[H_2SO_4]_0$ bracketing the oscillatory region. The pH values of both branches of steady states lie between the maximum and minimum pH of oscillation. The short plateau in the pH oscillation shown in Figure 1 occurs at a pH near that of the thermo branch steady state.

Component Processes

Reactants of the oscillatory Landolt reaction include iodate, sulfite, ferrocyanide, and hydrogen ion supplied by sulfuric acid. Following EOE,[15] we identify the major component processes of the reaction according to literature accounts of reactions between the primary reactants and reactions involving major intermediate species. Our scheme of component processes is similar to the scheme proposed by EOE.[15] In addition to the oxidation–reduction processes, we find that the stoichiometrically significant oxysulfur species constitute a buffer system that must be included in an ERL description of the oscillatory behavior.

Iodate Oxidation of Iodide. The major pathway for the reduction of iodate is the Dushman reaction[25] given by process A.

$$IO_3^- + 8I^- + 6H^+ = 3I_3^- + 3H_2O \qquad (A)$$

The stoichiometry of process A is written in terms of the product I_3^- rather than I_2 since, as shown in Figure 1, I^- is always present in relatively high concentration. While both I_2 and I_3^- appear as reactant species in other processes, they are in rapid equilibrium[26] and the stoichiometry of each process is written in terms of the predominant species I_3^-.

Process A has been the subject of many investigations since Dushman's 1904 study.[25] Liebhafsky and Roe[27] have reviewed the empirical rate laws that have appeared over the years. Many studies have found that a two-term rate law is necessary for an accurate description of the reaction.[28-30] A term first-order in iodide is dominant at low iodide concentrations; at higher iodide concentrations a second term second-order in iodide becomes dominant. The first-order term is difficult to characterize because in typical experiments even the iodide contaminant in the iodate reagent provides sufficient concentration to make the second-order term dominant. The second-order term, however, is well-established and was even reported in Dushman's original study.[25] Liebhafsky and Roe[27] concluded that rate law α is most consistent with the known experimental behavior. Rate law α has been an

$$R_\alpha = \frac{-d[IO_3^-]}{dt} = k_{\alpha 1}[IO_3^-][I^-][H^+]^2 + k_{\alpha 2}[IO_3^-][I^-]^2[H^+]^2 \qquad (\alpha)$$

essential component in the descriptions of bistability[5-10] and chemical waves[12,13] in the iodate–arsenous acid reaction. The disproportionation of I_2 in the reverse reaction is insignificant at the acidities of the oscillatory Landolt reaction, and process A is therefore considered to be irreversible.

Bisulfite Reduction of Iodine and Triiodide. Iodine and triiodide generated in process A react with bisulfite to generate iodide and bisulfate. While both HSO_3^- and SO_3^{2-} are stoichiometrically significant in typical experiments reported here and in those reported by EOE,[15] only HSO_3^- reacts with I_2 and I_3^- according to a study by Bünau and Eigen.[31] The net reaction is written in terms of triiodide ion according to process B.

$$HSO_3^- + I_3^- + H_2O = HSO_4^- + 3I^- + 2H^+ \qquad (B)$$

Bünau and Eigen[31] studied the sulfite reduction of iodine at different acidities and varying concentrations of iodide and chloride. Three reaction pathways were found, two corresponding to the bisulfite reductions of I_2 and I_3^- and the third corresponding to the reduction of I_2Cl^-. Rate law β, with the term for the reduction of I_2Cl^- omitted, is relevant to the experiments reported here. The second term includes the formation constant K for

$$R_\beta = \frac{-d[I_3^-]}{dt} = k_{\beta 1}[I_3^-][HSO_3^-] + \frac{k_{\beta 2}[I_3^-][HSO_3^-]}{K[I^-]} \qquad (\beta)$$

I_3^-. Rate law β indicates that HOI from the hydrolysis of I_2 is unimportant in the reaction; bisulfite is apparently sufficiently reactive to directly attack I_2 and I_3^-. Bünau and Eigen found no evidence for significant reverse reaction and process B is therefore regarded as irreversible.

Ferrocyanide Reduction of Iodine. The iodine product of process A may also be reduced by ferrocyanide. The protonated complex $HFe(CN)_6^{3-}$ ($pK_a = 4.2$)[32] is significant only briefly in the oscillatory Landolt reaction as the pH reaches its lowest values. We neglect the protonation and write the stoichiometry of the reaction according to process C.

$$2Fe(CN)_6^{4-} + I_3^- = 2Fe(CN)_6^{3-} + 3I^- \qquad (C)$$

A detailed investigation of process C by Reynolds[33] showed that the rate of oxidation of $Fe(CN)_6^{4-}$ in solutions containing I_2 and I_3^- depends inversely on the concentration of I^-, indicating reaction with I_2 and not with I_3^-. The complete rate law for the forward and reverse reactions can be expressed in terms of $Fe(CN)_6^{4-}$ by employing conservation of iron atoms.

$$R_\gamma = \frac{-d[I_3^-]}{dt} = \frac{k_\gamma[I_3^-][Fe(CN)_6^{4-}]^2}{K[I^-][Fe(CN)_6^{4-}]_0} - \frac{k_{-\gamma}([Fe(CN)_6^{4-}]_0 - [Fe(CN)_6^{4-}])^2[I^-]^2}{[Fe(CN)_6^{4-}]_0} \qquad (\gamma)$$

The reverse reaction between $Fe(CN)_6^{3-}$ and I^- has been studied more extensively than the forward reaction and has been found to be comparatively slow.[34-36]

Reynolds studied process C at pH 7.1 and 9.2 and found no pH dependence; however, less detailed studies of the reduction of I_2 with no added I^- showed that the reaction proceeds much slower at pH 1.48. While the oxidation of protonated ferrocyanide by I_2 is apparently slower, it seems likely that the reaction pathway involving the oxidation by I_3^- becomes more important at higher acidities as the charge on ferrocyanide is decreased in successive protonations.

Uncatalyzed Iodate Oxidation of Bisulfite. An uncatalyzed direct reaction between bisulfite and iodate involving successive oxygen atom transfers was proposed in the early studies of Landolt[2] and Eggert and Scharnow.[4] While the direct reaction between iodate and arsenous acid is very slow[4] and often considered to be negligible,[6-10,12] bisulfite is apparently sufficiently reactive that this pathway becomes significant. Evidence that the direct reaction is important with bisulfite and not with arsenous acid comes from the observation that slightly basic solutions containing bisulfite and iodate react fairly rapidly to completion[15,37] while similar solutions containing arsenous acid and iodate do not react over the course of days.[14] The stoichiometry of the direct reaction is the same as that of (A) + 3(B); however, the processes involve two distinct reaction pathways.

$$IO_3^- + 3HSO_3^- = I^- + 3HSO_4^- \qquad (D)$$

(25) Dushman, S. *J. Phys. Chem.* **1904**, *8*, 453.
(26) Myers, O. E. *J. Chem. Phys.* **1958**, *28*, 1027.
(27) Liebhafsky, H. A.; Roe, G. M. *Int. J. Chem. Kinet.* **1979**, *11*, 693.
(28) Abel, E.; Hilferding, K. *Z. Phys. Chem.* **1928**, *136*, 186.
(29) Beran, P.; Bruckenstein, S. *J. Phys. Chem.* **1968**, *72*, 3630.
(30) Schildcrout, S. M.; Fortunato, F. A. *J. Phys. Chem.* **1975**, *79*, 31.
(31) Bünau, G. V.; Eigen, M. *Z. Phys. Chem. N.F.* **1962**, *32*, 27.
(32) Jordan, J.; Ewing, G. J. *Inorg. Chem.* **1962**, *1*, 587.
(33) Reynolds, W. L. *J. Am. Chem. Soc.* **1958**, *80*, 1830.
(34) Adamson, A. W. *J. Phys. Chem.* **1952**, *56*, 858.
(35) Indelli, A.; Guaraldi, G. C. *J. Chem. Soc.* **1964**, 36.
(36) Majid, Y. A.; Howlett, K. E. *J. Chem. Soc. A* **1968**, 679.
(37) Sorum, C. H.; Charlton, F. S.; Neptune, J. A.; Edwards, J. O. *J. Am. Chem. Soc.* **1952**, *74*, 219.

Table II. Rate and Equilibrium Constants for Model N

$k_{\alpha 1} = 9.2 \times 10^5\ M^{-3}\ s^{-1}$	$k_{\alpha 2} = 8.1 \times 10^8\ M^{-4}\ s^{-1}$
$k_{\beta 1} = 2.2 \times 10^7\ M^{-1}\ s^{-1}$	$k_{\beta 2} = 2.3 \times 10^9\ M^{-1}\ s^{-1}$
$k_{-\gamma}{}^a = (1.3 \times 10^3\ M^{-1}\ s^{-1})$	$k_{-\gamma}{}^a = (6.1 \times 10^{-3}\ M^{-2}\ s^{-1})$
$k_\gamma{}^b = 8.5 \times 10^4\ M^{-1}\ s^{-1}$	
$k_\delta = 0.25\ M^{-1}\ s^{-1}$	
$k_{\epsilon 1} = 3.4 \times 10^6\ s^{-1}$	$k_{-\epsilon 1} = 2.0 \times 10^8\ M^{-1}\ s^{-1}$
$k_{\epsilon 2} = 8.1 \times 10^3\ s^{-1}$	$k_{-\epsilon 2} = 5.0 \times 10^{10}\ M^{-1}\ s^{-1}$
$k_{\epsilon 3} = 2.5 \times 10^9\ s^{-1}$	$k_{-\epsilon 3} = 1.0 \times 10^{11}\ M^{-1}\ s^{-1}$
$K = 539\ M^{-1}$	

[a] Values used in Figure 4. [b] Value used in Figures 3 and 5.

Rate measurements of process D are difficult because the alternate autocatalytic pathway (A) + 3(B) is usually dominant. Thus, while process D is usually included in descriptions of the Landolt reaction, the form of the rate law and corresponding rate constant(s) have not been experimentally determined. An early study by Skrabal and Zahorka[38] reported a high-order two-term rate law; however, there is considerable uncertainty in their interpretation. We describe process D as a simple bimolecular reaction between IO_3^- and HSO_3^- according to rate law δ followed by rapid oxygen atom transfers.[2,4]

$$R_\delta = \frac{-d[IO_3^-]}{dt} = k_\delta[IO_3^-][HSO_3^-] \qquad (\delta)$$

Buffer System. The reactant and product oxysulfur species constitute a buffer system that is continually titrated by the oxidation–reduction reactions. In turn the solution pH established by the buffer system dramatically affects the redox chemistry. The proton equilibria that are significant over the experimental pH range are given by reactions E.[39] The major S(IV) species

$$H_2SO_3 = H^+ + HSO_3^- \qquad (E1)$$

$$HSO_3^- = H^+ + SO_3^{2-} \qquad (E2)$$

$$HSO_4^- = H^+ + SO_4^{2-} \qquad (E3)$$

are H_2SO_3, HSO_3^-, and SO_3^{2-}, all in rapid equilibrium. The S(VI) species HSO_4^- and SO_4^{2-} are also important in the buffer system because sulfite is partially acidified in the reactant stream with sulfuric acid and the primary oxidation product of the reaction is S(VI). We neglect the protonation of ferrocyanide because its concentration in the reaction mixture is insufficient to significantly affect the buffer system. Empirical rate laws for reactions E1–E3 are obtained directly from the elementary steps.

$$R_{\epsilon 1} = \frac{-d[H_2SO_3]}{dt} = k_{\epsilon 1}[H_2SO_3] - k_{-\epsilon 1}[H^+][HSO_3^-] \qquad (\epsilon 1)$$

$$R_{\epsilon 2} = \frac{-d[HSO_3^-]}{dt} = k_{\epsilon 2}[HSO_3^-] - k_{-\epsilon 2}[H^+][SO_3^{2-}] \qquad (\epsilon 2)$$

$$R_{\epsilon 3} = \frac{-d[HSO_4^-]}{dt} = k_{\epsilon 3}[HSO_4^-] - k_{-\epsilon 3}[H^+][SO_4^{2-}] \qquad (\epsilon 3)$$

Empirical Rate Law Model

We now develop an empirical rate law model based on the component processes presented above. Each variable species is described by a differential equation in terms of the stoichiometry of each component process and the corresponding rate law. Each differential equation includes the term $-k_0[C_i]$ for the removal of species C_i from the reactor by the outflow, where k_0 is the reciprocal residence time (flow rate/tank volume) and is equivalent to a first-order rate constant. The input of reactants is described by including the term $k_0[C_i]_0$ in the differential equations for these species, where $[C_i]_0$ is the concentration of C_i in the combined reactant stream. The empirical rate law model is made up of the differential equations N1–N10 for the ten variable species. The

$$\frac{d[IO_3^-]}{dt} = -R_\alpha - R_\delta + k_0([IO_3^-]_0 - [IO_3^-]) \qquad (N1)$$

$$\frac{d[I^-]}{dt} = -8R_\alpha + 3R_\beta + 3R_\gamma + R_\delta + k_0([I^-]_0 - [I^-]) \qquad (N2)$$

$$\frac{d[I_3^-]}{dt} = 3R_\alpha - R_\beta - R_\gamma - k_0[I_3^-] \qquad (N3)$$

$$\frac{d[Fe(CN)_6^{4-}]}{dt} = -2R_\gamma + k_0([Fe(CN)_6^{4-}]_0 - [Fe(CN)_6^{4-}]) \qquad (N4)$$

$$\frac{d[H^+]}{dt} = -6R_\alpha + 2R_\beta + R_{\epsilon 1} + R_{\epsilon 2} + R_{\epsilon 3} + k_0([H^+]_0 - [H^+]) \qquad (N5)$$

$$\frac{d[H_2SO_3]}{dt} = -R_{\epsilon 1} - k_0[H_2SO_3] \qquad (N6)$$

$$\frac{d[HSO_3^-]}{dt} = -R_\beta - 3R_\delta + R_{\epsilon 1} - R_{\epsilon 2} - k_0[HSO_3^-] \qquad (N7)$$

$$\frac{d[SO_3^{2-}]}{dt} = R_{\epsilon 2} + k_0([SO_3^{2-}]_0 - [SO_3^{2-}]) \qquad (N8)$$

$$\frac{d[HSO_4^-]}{dt} = R_\beta + 3R_\delta - R_{\epsilon 3} + k_0([HSO_4^-]_0 - [HSO_4^-]) \qquad (N9)$$

$$\frac{d[SO_4^{2-}]}{dt} = R_{\epsilon 3} - k_0[SO_4^{2-}] \qquad (N10)$$

input of H_2SO_4 is accounted for by equal concentrations of H^+ and HSO_4^- in the reactant stream. The input of I^- in (N2) is included to account for the impurity in iodate reagent. The total number of species in model N is actually 11, but conservation of iron atoms in rate law γ allowed elimination of $Fe(CN)_6^{3-}$ as a variable. Conservation of iodine atoms and sulfur atoms with similar modifications of the corresponding rate laws would allow the model to be reduced to 8 variable species.

Rate Constant Assignments. Because the oscillatory behavior is robust and readily reproducible at 40.0 °C, values of the rate and equilibrium constants were selected for this temperature when possible. (See Table II for rate and equilibrium constants described below.)

Values of $k_{\alpha 1}$ and $k_{\alpha 2}$ in rate law α were obtained from a study of the temperature dependence of process A by Schildcrout and Fortunato.[30] Apparent activation energies for the rate constants were used with values measured at 25.0 °C to determine values for 40.0 °C.

Values for $k_{\beta 1}$ and $k_{\beta 2}$ in rate law β were taken from the investigation by Bünau and Eigen.[31] The temperature dependence of this very fast reaction has not been studied; however, because it is expected to be small, we use the rate constants measured at 22.0 °C. The formation constant K for triiodide, which appears in rate laws β and γ, was obtained from a temperature-dependence study of the equilibrium by Burger and Liebhafsky.[40] The value of K for 40.0 °C was calculated from the value measured at 25.0 °C and $\Delta H°$ for the reaction.

Rate constants k_γ and $k_{-\gamma}$ for the forward and reverse reactions of process C were taken from Reynolds.[33] No measurements of the temperature dependence of process C are available, and we therefore use the values measured at 24.0 °C (in parentheses in Table II) in our initial modeling attempt.

No rate constant for process D is available from the literature; therefore, the value of k_δ was estimated by fitting measurements carried out by EOE[15] of the "Landolt time" for the appearance of iodine in batch reaction. Process C was omitted from model N in these calculations, and 25.0 °C values for $k_{\alpha 1}$, $k_{\alpha 2}$, and K

(38) Skrabal, A.; Zahorka, A. *Z. Elektrochem.* **1927**, *33*, 42.
(39) Smith, R. M.; Martell, A. E. *Critical Stability Constants*; Plenum Press: New York, 1976; Vol. 4.
(40) Burger, J. D.; Liebhafsky, H. A. *Anal. Chem.* **1973**, *45*, 600.

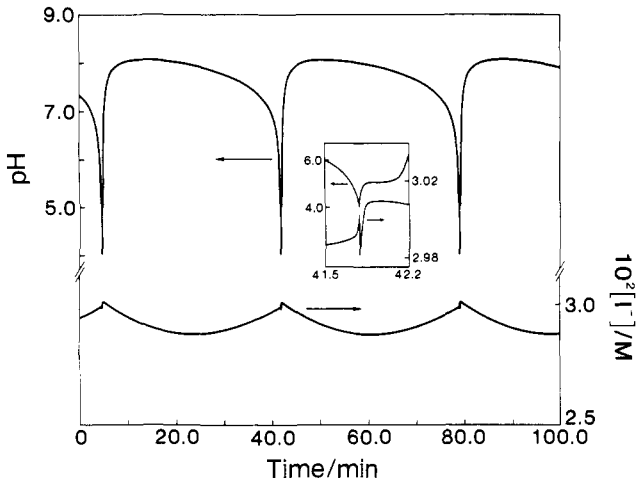

Figure 4. Iodide concentration (below) and pH (above) as a function of time calculated from model N. Reactant stream concentrations given in Table I except $[H_2SO_4]_0 = 1.0 \times 10^{-3}$ M. Rate constants in Table II and $k_0 = 1.0 \times 10^{-4}$ s^{-1}. Inset shows blowup of iodide concentration (below) and pH (above) between 41.5 and 42.2 min.

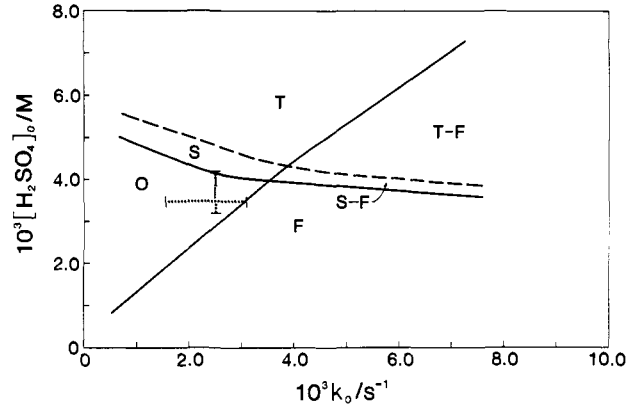

Figure 5. Kinetic phase diagram in the constraints $[H_2SO_4]_0$ and k_0 calculated from model N. Flow branch monostability (F), thermo branch monostability (T), steady-state bistability (T–F), small-amplitude oscillations (S), small-amplitude oscillations–flow branch bistability (S–F), and large-amplitude oscillations (O). Reactant stream concentrations in Table I and rate constants in Table II. Dotted lines show experimental range in k_0 and $[H_2SO_4]_0$ of large-amplitude oscillations.

were used to better correspond to the 30.0 °C measurements.

Rate constants for reactions E1 and E3 of the buffer system are available;[41,42] however, rate constants for reaction E2 have not been measured. The reverse rate constant $k_{-\epsilon 2}$ was assigned a value of half the measured value of $k_{-\epsilon 3}$ because the lower value is more typical of similar proton transfer reactions.[43] The forward rate constant $k_{\epsilon 2}$ was calculated from the value of the equilibrium constant[39] and $k_{-\epsilon 2}$. No measurements of the temperature dependence of the rate constants for reactions E1–E3 are available; however, the corresponding values[39] of $\Delta H°$ predict decreases of only 22%, 28%, and 36% in the equilibrium constants K_{E1}, K_{E2}, and K_{E3} when the temperature is increased from 25.0 °C to 40.0 °C. Because the fast reverse reactions will be relatively insensitive to temperature changes, the forward rate constants will reflect the variations in the equilibrium constants. However, the variations are sufficiently small that no temperature corrections were attempted and the 25.0 °C values listed in Table II were used in our calculations.

Calculated Behavior

The differential equations of model N with the rate constants listed in Table II were numerically integrated with use of the Gear algorithm.[44] Our first calculations included only processes A–D without the buffer system of reactions E. No oscillatory behavior was found in these calculations throughout an extensive scan of flow rates and reactant concentrations. When reactions E were included in the model, oscillatory behavior was quickly found at lower values of k_0 and $[H_2SO_4]_0$. No oscillations were found, however, with the values of k_0 and $[H_2SO_4]_0$ used in Figure 1. Shown in Figure 4 is an example of oscillations in pH and iodide concentration calculated with $k_0 = 1.0 \times 10^{-4}$ s^{-1} and reactant concentrations the same as in Figure 1 except $[H_2SO_4]_0 = 1.0 \times 10^{-3}$ M. Only the qualitative behavior can be compared in Figures 1 and 4 since the values of k_0 and $[H_2SO_4]_0$ differ; however, we see that the major features including the sharp minimum and brief plateau in the pH curve are well-reproduced by the model calculations. The almost constant iodide concentration is also reproduced; however, the sharp negative spike is much less pronounced than in the experimental measurements.

Calculations carried out to determine the values of $[H_2SO_4]_0$ and k_0 where oscillatory behavior is exhibited yielded a cross-shaped phase diagram[16,17] showing the regions of monostability, bistability, and oscillatory behavior in these constraints. The critical (cross) point where oscillatory behavior gives way to bistability occurs at about $[H_2SO_4]_0 = 9.0 \times 10^{-4}$ M and $k_0 = 7.0 \times 10^{-4}$ s^{-1}, an order of magnitude lower in each constraint from that expected according to our experiments and those of EOE.[15]

Convinced by these calculations that the major dynamical features of the oscillatory Landolt reaction are accounted for by model N, better quantitative agreement with experiment was sought while maintaining the objective of modeling with as few adjustable parameters as possible. An examination of processes A–E suggests that the rate constants for the iodine oxidation of ferrocyanide in process C are the most likely candidates for adjustment. The differences in pH and temperature between our experiments and those of Reynolds[33] indicate that the reported values are not appropriate for the oscillatory Landolt reaction.

Calculations carried out to determine the importance of the reverse reaction in process C showed little change in amplitude of the pH oscillations and less than 1.0% change in period when $k_{-\gamma}$ was set to 0 in the calculation for Figure 4. Because the relatively slow reverse reaction of process C does not significantly affect the behavior, this process was considered to be irreversible in the remaining calculations.

Adjustments of k_γ showed that the experimental range of oscillatory behavior in Figure 3 could be reasonably well matched by increasing its value by a factor of about 65. In this calculation, the value of k_0 and the reactant concentrations matched the experimental values; only the value of k_γ was adjusted (Table II). The calculated period and amplitude of the pH oscillations and the steady-state pH values are shown in Figure 3. While the calculated period as a function of $[H_2SO_4]_0$ is slightly higher than that found in experiment, the qualitative features are well-matched. In both experiment and calculation, the period increases as $[H_2SO_4]_0$ is decreased to the bifurcation point where the flow branch steady state emerges. The amplitude of oscillation along with the relative positions of the flow and thermo branch steady states bracketing the oscillatory region are also in good agreement.

A feature predicted by the calculations but not found in the experimental measurements is the precipitous drop in the period from about 12.0 min at $[H_2SO_4]_0 \approx 4.1 \times 10^{-3}$ M to about 3.0 s at $[H_2SO_4]_0 \approx 4.2 \times 10^{-3}$ M. Accompanying this decrease in period by a factor of over 200 is a decrease in amplitude by almost 50-fold. As $[H_2SO_4]_0$ is further decreased from this apparent bifurcation, the period remains fairly constant and the amplitude decreases to zero at an apparent supercritical Hopf bifurcation at $[H_2SO_4]_0 \approx 4.6 \times 10^{-3}$ M. The small-amplitude oscillations were apparently not detectable by our electrode measurements because of their extremely short period. This explanation is supported by the observation that measurements of the thermo branch steady state near this bifurcation were particularly difficult;

(41) Eigen, M.; Kustin, K.; Maass, G. *Z. Phys. Chem. N.F.* **1961**, *30*, 130.
(42) Eigen, M.; Kurtze, G.; Tamm, K. *Z. Elektrochem.* **1953**, *57*, 103.
(43) Eigen, M.; Kruse, W.; Maass, G.; De Maeyer, L. In *Progress in Reaction Kinetics*; Porter, G., Ed.; MacMillan: New York, 1964; Vol. 2, pp 306–313.
(44) Hindmarsh, A. C. *Livermore Solver of Ordinary Differential Equations (LSODE)*; Lawrence Livermore Laboratory: Livermore, CA, 1980.

rapid fluctuations and drift in pH were repeatedly encountered.

Figure 5 shows a kinetic phase diagram in the constraints $[H_2SO_4]_0$ and k_0 predicted by model N for the reactant concentrations and rate constants used in Figure 3. Shown in the diagram are regions of large-amplitude oscillations (O), small-amplitude oscillations (S), flow branch (F) and thermo branch (T) monostability, steady-state bistability (T–F), and bistability between small-amplitude oscillations and the flow branch steady state (S–F). The regions can be viewed in terms of a cross-shaped diagram[16,17] separating the large-amplitude oscillations from the bistability region. Superimposed on the "normal" diagram is a band of small-amplitude oscillations separating the large-amplitude oscillations from the thermo branch and a band of steady-state-oscillation bistability separating the steady-state bistability from the flow branch.

The range in $[H_2SO_4]_0$ of large-amplitude oscillations corresponding to the measurements in Figure 3 is shown by the dotted vertical line. The horizontal dotted line shows the experimental range in k_0 for $[H_2SO_4]_0 = 3.5 \times 10^{-3}$ M. We see that the calculations predict large-amplitude oscillations at much lower values of k_0 than found experimentally. Spot checks of experimental behavior as a function of $[H_2SO_4]_0$ and k_0 showed generally poor agreement with the calculated regions in Figure 5. For example, large-amplitude oscillations were found within the calculated regions of small-amplitude oscillations, bistability, and steady-state-oscillation bistability.

Additional calculations were carried out to determine if better agreement between experiment and calculation could be obtained. The ferricyanide oxidation of sulfite was proposed by EOE[15] as a component process; however, this reaction was not included in model N because it is relatively slow.[45-47] To check our decision to omit this reaction, calculations were carried out with it included in model N according to the stoichiometry of process T and rate law θ.[45-47] Conservation of iron atoms allows rate law θ to be

$$2Fe(CN)_6^{3-} + SO_3^{2-} + H_2O = 2Fe(CN)_6^{4-} + SO_4^{2-} + 2H^+ \quad (T)$$

$$R_\theta = \frac{-d[SO_3^{2-}]}{dt} = k_\theta([Fe(CN)_6^{4-}]_0 - [Fe(CN)_6^{4-}])[SO_3^{2-}] \quad (\theta)$$

written in terms of $Fe(CN)_6^{4-}$. A calculation was carried out with reactant concentrations and rate constants the same as in Figure 3 with $[H_2SO_4]_0 = 3.5 \times 10^{-3}$ M and the value of k_θ (1.0×10^{-3} M^{-1} s^{-1}) taken from Swinehart.[47] No perceivable change in amplitude of the pH oscillations was found and the period changed by less than 1.0% compared to the calculation without process T. We conclude that the ferricyanide–sulfite reaction is not of major importance in the dynamics of the oscillatory Landolt reaction.

Other calculations involving adjustments of k_β, k_γ, and k_δ showed that the quantitative features of the phase diagram are sensitive to these rate constants and that the regions of behavior can be readily shifted. The qualitative features of the diagram, however, appear to be robust. Further adjustments of rate constants to obtain better agreement with the experimental behavior seemed inconsistent with the goal of describing the system in terms of experimentally established rate laws and rate constants and was not pursued.

Discussion

A simple modification of the venerable Landolt clock reaction, the introduction of ferrocyanide as an additional reducing agent, results in a fascinating oscillatory reaction when carried out in a CSTR. This new oscillatory reaction is an attractive system for analysis because it can be described in terms of component processes, many of which are well-characterized.

Comparison of Experimental and Calculated Behavior. Four stoichiometric processes representing component redox reactions and a buffer system arising from five oxysulfur species have been used to describe the oscillatory Landolt reaction. The rate behavior of all but one of the processes is characterized by experimentally established rate laws and associated rate and equilibrium constants. With only temperature corrections of the measured constants, oscillatory behavior and bistability are readily generated by the empirical rate law model. The calculated pH waveform is remarkably similar to the measured waveform. The pH oscillations (Figures 1 and 4) are characterized by a broad maximum followed by a sharp minimum with the subsequent rapid rise briefly interrupted by a short plateau. The major characteristic of the measured and calculated iodide concentration is that it is nearly constant, varying little from its rather high value. The fine structure of the measured iodide waveform is not matched by the calculations; however, many qualitative features are in good agreement. The first maximum in iodide concentration nearly coincides with the pH minimum in both experiment and calculation (see inset in Figure 4). A sharp negative spike is exhibited while the pH rises to the short plateau and a second maximum coincides with the pH plateau. The relative magnitudes of the first and second iodide maxima are reversed from the measured values and the negative spike occurs on a much shorter time scale than that observed experimentally. These discrepancies apparently result from inappropriate relative and absolute rates of processes B and C, as discussed below. A more serious discrepancy is the failure of model N to generate oscillatory behavior at values of $[H_2SO_4]_0$ and k_0 where oscillations are found experimentally.

Adjustment of rate constant k_γ for the I_2 oxidation of $Fe(CN)_6^{4-}$, seemingly the least reliable value for the conditions of the oscillatory Landolt reaction, results in good agreement with the measured range, period, and amplitude of oscillation as a function of $[H_2SO_4]_0$. In addition, a secondary bifurcation is predicted that gives rise to high-frequency, small-amplitude oscillations which seems to explain earlier experimental difficulties in characterizing an apparent steady state. The calculations predict three bifurcations as the system moves from the thermo branch to the flow branch upon decreasing $[H_2SO_4]_0$. The first has the features of a supercritical Hopf bifurcation; the second is an unusual transition from one oscillatory behavior to another; and the third has features of a saddle-node or saddle-loop bifurcation with period lengthening and nearly constant amplitude. A characterization of these bifurcations must await a more detailed experimental study and further refinement of the model.

While the dependence of the behavior on $[H_2SO_4]_0$ at a particular value of k_0 is well-described by model N, the calculated regions of bistability and oscillatory behavior in the $[H_2SO_4]_0$–k_0 constraint plane are in poor agreement with experiment. Oscillations are found at much higher values of $[H_2SO_4]_0$ and k_0 than predicted by the model calculations. The major qualitative features in Figure 5, however, should remain intact as refinements are made in the model.

In comparing the experimental and calculated behavior, the reliability of the experimental measurements must also be considered. An experimental constraint yet to be examined in this system is the effect of stirring rate on the behavior. A number of recent studies have demonstrated that mixing effects may play an important role in determining the behavior of bistable and oscillatory systems.[48-50] An indication that mixing effects might be important in this system is that our measurements of the pH oscillations showed the short plateau behavior while this behavior was not observed in the experiments of EOE.[15] If the system is sensitive to stirring rate, it is likely that regions of behavior in the kinetic phase diagram will be shifted as mixing is improved.

Limitations and Refinements of the Empirical Rate Law Model. A potentially serious deficiency in any empirical rate law model is the possible coupling of component processes beyond that described by the model. The intermediate species of one process

(45) Higginson, W. C. E.; Marshall, J. W. *J. Chem. Soc.* **1957**, 447.
(46) Vepřek-Šiška, J.; Hasnedl, A. *Chem. Commun.* **1968**, 1167.
(47) Swinehart, J. H. *J. Inorg. Nucl. Chem.* **1967**, *27*, 2313.
(48) Roux, J. C.; De Kepper, P.; Boissonade, J. *Phys. Lett.* **1983**, *A97*, 168.
(49) Kumpinsky, E.; Epstein, I. R. *J. Chem. Phys.* **1985**, *82*, 53.
(50) Menzinger, M.; Boukalouch, M.; De Kepper, P.; Boissonade, J.; Roux, J. C.; Saadaoui, H. *J. Phys. Chem.* **1986**, *90*, 313.

may react with the species of another process and thereby affect the rate behavior of either or both processes. The success of an ERL model depends on minimal mixing of the component processes.

The qualitative agreement between experiment and calculation shown in Figures 1, 3, and 4 is strong evidence that the major dynamical features of the system are described by model N. The lack of agreement between the experimental and calculated regions of behavior is disturbing; however, a search for quantitative agreement by adjusting the (empirical) rate constants seems inappropriate. A rational approach for refinement of the model and the experimental description of the system is to experimentally reexamine the least well characterized component processes.

The rate constants reported[33] for process C are apparently inappropriate for modeling the oscillatory Landolt reaction. Rate parameters for this process must be obtained from experiments carried out at 40.0 °C with mildly acidic solutions containing excess iodide. While process B seems to be well-characterized,[31] the very sharp first maximum in iodide concentration (Figure 4 inset) suggests that the calculated rate of this process is too rapid to reproduce the experimental behavior. Results of another study[51] indicate that the very rapid reaction might pertain to the formation of the intermediate species which then decays at a slower rate. Process D is the least well characterized component of model N. Even the form of the rate law for this process is uncertain; however, because its role is relegated to initiating each cycle of oscillation at the broad pH maximum, its primary importance is in determining the period of oscillation. Insight into process D can be obtained by measuring the Landolt time for the appearance of I_2 in initially neutral solutions containing iodate and sulfite. In these solutions, the long induction period will be primarily determined by process D since the rate of the Dushman reaction is negligible until the pH suddenly decreases near the end of the period.

Detailed Mechanism. Insight into the oscillatory behavior can be gained by considering the different phases of the oscillatory cycle in terms of the processes of model N. Iodide and hydrogen ion are generated autocatalytically by the sequence (A) + 3(B) as the pH falls from its maximum (Figure 4). Because process A is much slower than process B, the rate of reaction is governed by rate law α. Bisulfite and the other S(IV) species in rapid equilibrium are depleted at the pH minimum; iodide and hydrogen ion autocatalysis is terminated because process B is no longer possible. Iodide continues to react with iodate, however, and the result is a sudden decrease in iodide concentration accompanied by a sudden rise in pH according to the stoichiometry of process A (Figure 4 inset). As I_2 is generated by the Dushman reaction, process C becomes important and I^- concentration again increases autocatalytically by the sequence (A) + 3(C). Hydrogen ion, however, is consumed in this sequence and pH continues to rise. The plateau in pH and the second maximum in I^- concentration result from the depletion of I_2 and the termination of sequence (A) + 3(C). This feature does not result from a depletion of $Fe(CN)_6^{4-}$ because the concentration of this species remains within 70% of the input concentration throughout the cycle. The subsequent increase in pH and decrease in I^- concentration result from a combination of process A and washout from the reagent flow; the rate of the Dushman reaction, however, sharply diminishes as pH increases. The flow of slightly basic reagent into the reactor is also important in the pH increase. Reaction sequences that depend on process A cannot occur as the pH nears its maximum; therefore, the initiation of the next cycle depends on the direct reaction of IO_3^- with HSO_3^- in process D.

We now present a detailed mechanism of the oscillatory Landolt reaction in terms of elementary and pseudoelementary steps, consistent with the stoichiometry and empirical rate laws of model N. The mechanism is listed in Table III with each sequence of steps identified with a component process of model N.

The mechanism for the Dushman reaction (process A) has long been a subject of debate because of the unusual second-order dependence in iodide. Bray[52] proposed a reaction scheme in 1930 that accounted for the fourth- and fifth-order, two-term rate law. His convincing argument called for preequilibrium 1 followed by the rate-determining steps 2 and 3. The critical intermediate species in this scheme is $H_2I_2O_3$ or I_2O_2, the mixed anhydride of HOI and HIO_2. Decomposition of the intermediate in step 2 leads to the fourth-order term and bimolecular reaction with I^- in step 3 leads to the fifth-order term. The resulting HOI and HIO_2 rapidly react with I^- to generate I_2 which in excess I^- leads to I_3^-. This scheme was formulated in collaboration with Liebhafsky[52] and almost 50 years later Liebhafsky and Roe[27] refined the mechanism in a numerical simulation of the Dushman reaction. Liebhafsky and Roe's mechanism combined with Roebuck's[53] mechanism for the H_3AsO_3 reduction of I_2 has been used to accurately model bistability in the iodate–arsenous acid reaction.[6] The net reaction for process A is given by 2(1) + (2) + (3) + (4) + (5) + 6(6) + 6(7).

Bünau and Eigen[31] studied process B using flow techniques and proposed a reaction mechanism involving the steady state intermediate HSO_3I. At the concentrations of I^- typical in the oscillatory Landolt reaction, step 10 of the two-pathway scheme is rate determining and the steady-state rate law simplifies to rate law β. The steady-state rate law and rate law β result in apparent rate constants that agree within 1% at these iodide concentrations. The net reaction for process B is given by (−7) + (8) + (9) + 2(10).

A mechanism involving the steady-state intermediate I_2^- was proposed by Reynolds[33] for process C. Rate law γ corresponds to this steady-state scheme when rate constants k_{-11} and k_{12} are nearly equal. The net reaction for process C is given by (−7) + (11) + (12).

A mechanism involving successive oxygen atom transfers from the oxyiodine species to bisulfite is proposed for process D, following Landolt[2] and Eggert and Scharnow.[4] Rate law δ corresponds to step 13 being rate determining followed by rapid steps 14 and 15. The net reaction for process D is given by (13) + (14) + (15) + (−18), where the last step is a proton-transfer reaction.

There is significant overlap in the schemes for the autocatalytic sequence (A) + 3(B) and process D. Reactions 14 and 15 could be important following the rate-determining steps 2 and 3 in process A. This would lead to two pathways for the reduction

Table III. Detailed Mechanism

Process A	
$IO_3^- + I^- + 2H^+ \rightleftarrows H_2I_2O_3$	(1)
$H_2I_2O_3 \rightarrow HOI + HIO_2$	(2)
$H_2I_2O_3 + I^- \rightarrow 2HOI + OI^-$	(3)
$OI^- + H^+ \rightleftarrows HOI$	(4)
$I^- + HIO_2 + H^+ \rightleftarrows 2HOI$	(5)
$I^- + HOI + H^+ \rightleftarrows I_2 + H_2O$	(6)
$I_2 + I^- \rightleftarrows I_3^-$	(7)
Process B	
$I_3^- \rightleftarrows I^- + I_2$	(−7)
$HSO_3^- + I_2 \rightleftarrows HSO_3I + I^-$	(8)
$HSO_3^- + I_3^- \rightleftarrows HSO_3I + 2I^-$	(9)
$HSO_3I + H_2O \rightarrow HSO_4^- + I^- + 2H^+$	(10)
Process C	
$I_3^- \rightleftarrows I^- + I_2$	(−7)
$Fe(CN)_6^{4-} + I_2 \rightleftarrows Fe(CN)_6^{3-} + I_2^-$	(11)
$Fe(CN)_6^{4-} + I_2^- \rightleftarrows Fe(CN)_6^{3-} + 2I^-$	(12)
Process D	
$IO_3^- + HSO_3^- \rightarrow HIO_2 + SO_4^{2-}$	(13)
$HIO_2 + HSO_3^- \rightarrow HOI + HSO_4^-$	(14)
$HOI + HSO_3^- \rightarrow I^- + HSO_4^- + H^+$	(15)
Buffer System	
$H_2SO_3 \rightleftarrows H^+ + HSO_3^-$	(16)
$HSO_3^- \rightleftarrows H^+ + SO_3^{2-}$	(17)
$HSO_4^- \rightleftarrows H^+ + SO_4^{2-}$	(18)

(51) Inoue, H.; Sudo, Y. *Kogyo Kagaku Zasshi* **1967**, *70*, 123.

(52) Bray, W. C. *J. Am. Chem. Soc.* **1930**, *52*, 3580.

(53) Roebuck, J. R. *J. Phys. Chem.* **1902**, *6*, 365.

of HOI and HIO_2 to generate I^-; however, the rate law and stoichiometry of the overall sequence would remain the same. Similarly, reactions 5-10 could be important in the further reduction of HIO_2 in process D. Again, two pathways would result without affecting the rate law and stoichiometry. We note that Bünau and Eigen[33] did not find evidence for a pathway involving HOI in process B, suggesting that the sequence 14-15 is not dominant.

Reactions 16-18 for the buffer system are reversible elementary steps for dissociation of the respective weak acids.

Conclusion

The oscillatory Landolt reaction is an important new addition to the growing list of oscillatory chemical systems.[17] Because the reaction can be described in terms of experimentally accessible component processes, an empirical characterization of the dynamical behavior is possible. The major qualitative features of the system are well-described by the empirical rate law model developed here. Quantitative agreement between calculation and experiment must await further refinement of the model and a better characterization of the experimental behavior. A detailed mechanism for the reaction has been developed by combining previously proposed schemes for the individual component processes.

Acknowledgment. This work was supported by the National Science Foundation (Grant No. CHE-8613240).

A Mechanism for Dynamical Behavior in the Landolt Reaction with Ferrocyanide[1]

Elizabeth C. Edblom,[†] László Györgyi,[‡] Miklós Orbán,[‡] and Irving R. Epstein*[†]

Contribution from the Department of Chemistry, Brandeis University, Waltham, Massachusetts 02254, and Institute of Inorganic and Analytical Chemistry, L. Eötvös University, H-1443 Budapest, Hungary. *Received February 3, 1987*

Abstract: A mechanism consisting of 13 elementary steps is proposed for the reaction of iodate, sulfite, and ferrocyanide. Computer simulations with the mechanism give excellent agreement with experimental observations of the batch behavior of both the component Landolt (iodate–sulfite) and the full system and with the bistability and oscillation found with the full system in a stirred tank reactor.

One of the most remarkable outcomes of the study of chemical oscillation has been the ability of chemists to construct, given data on the time variation of the concentration of one or two species, complex mechanisms involving a dozen or more elementary steps whose predictions yield excellent agreement with a wide variety of observed dynamical behavior. The best known example of such an achievement is the Field–Körös–Noyes mechanism[2] for the Belousov–Zhabotinskii reaction. Other oscillating reactions for which mechanisms in substantial agreement with experiment are available include the Bray–Liebhafsky,[3] chlorite–iodide,[4] and bromate–iodide[5] reactions.

Edblom, Orbán, and Epstein (EOE)[6] recently found that the reaction of iodate, sulfite, and ferrocyanide exhibits both bistable and oscillatory behavior in an open system. This modified Landolt reaction[7] appears tailor-made for mechanistic studies, since it allows for measurement of an unprecedented number of species concentrations. Ion-selective and pH electrodes can be used to monitor $[H^+]$ and $[I^-]$. The iodine concentration can be measured spectrophotometrically, and both ferro- and ferricyanide ions absorb in the visible. The very high extinction coefficients of the latter species have hampered quantitative studies of their behavior to date, but considerable qualitative information has been obtained.

We present here a mechanism for the Landolt reaction with ferrocyanide. The basic outlines of the mechanism were suggested by EOE in their experimental study of this system. Here we expand those ideas into a detailed mechanism consisting of 13 elementary steps. When this study was nearly complete, we became aware of an independent investigation by Gáspár and Showalter.[8] Their mechanism, though it focuses primarily on a set of empirical rate laws rather than on the component elementary steps, resembles the present one in all major respects. The striking similarity between two mechanisms arrived at independently and by different routes recalls a similar occurrence in the development of a mechanism for the Briggs–Rauscher oscillating reaction[9,10] and lends support to the mechanisms proposed.

Experimental Background

The experimental data to be considered are those obtained by EOE.[6] In summary, the simple Landolt (iodate–sulfite) reaction behaves as a clock reaction in a closed (batch) system,[11] showing a rapid drop in pH and a sharp rise in redox potential followed by a slower increase in pH accompanied by a constant redox potential and the production of I_2. In a stirred tank reactor (CSTR), the Landolt reaction exhibits bistability between a high pH, low redox potential, low I_2 steady state stable at high flow rates and a low pH, high potential, high I_2 state stable at low flow rates. No oscillations were observed in this reaction at any temperature.

The mixed system obtained by adding ferrocyanide to the components of the Landolt reaction behaves rather differently. The batch behavior is changed only slightly, in that the brown iodine color that persists after the sharp pH change in the Landolt reaction appears only transiently in the mixed system. The differences in the CSTR are more significant. At 20 °C, the mixed system is bistable over a considerably narrower range of flow rates than the Landolt reaction and the difference in redox potential between the two steady states is only about 100 mV compared

[†] Brandeis University.
[‡] L. Eötvös University.

(1) Part 41 in the series Systematic Design of Chemical Oscillators. Part 40: Simoyi, R. H.; Epstein, I. R. *J. Phys. Chem.*, in press.
(2) Field, R. J.; Körös, E.; Noyes, R. M. *J. Am. Chem. Soc.* **1972**, *94*, 8649.
(3) Sharma, K. R.; Noyes, R. M. *J. Am. Chem. Soc.* **1976**, *98*, 4345.
(4) Epstein, I. R.; Kustin, K. *J. Phys. Chem.* **1985**, *89*, 2275.
(5) Citri, O.; Epstein, I. R. *J. Am. Chem. Soc.* **1986**, *108*, 357.
(6) Edblom, E. C.; Orbán, M.; Epstein, I. R. *J. Am. Chem. Soc.* **1986**, *108*, 2826.
(7) Landolt, H. *Ber. Dtsch. Chem. Ges.* **1886**, *19*, 1317.
(8) Gáspár, V.; Showalter, K. *J. Am. Chem. Soc.*, preceding paper in this issue.
(9) Noyes, R. M.; Furrow, S. D. *J. Am. Chem. Soc.* **1982**, *104*, 45.
(10) De Kepper, P.; Epstein, I. R. *J. Am. Chem. Soc.* **1982**, *104*, 49.
(11) Eggert, J.; Scharnow, B. *Z. Elektrochem.* **1921**, *27*, 45.

0002-7863/87/1509-4876$01.50/0